

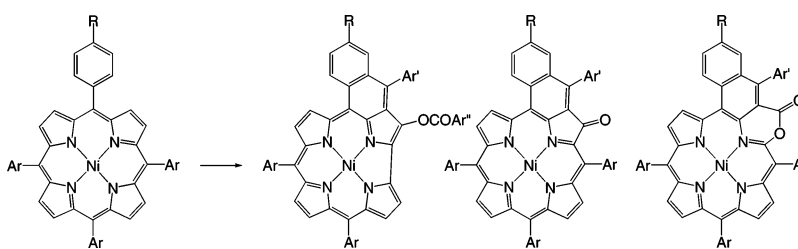
## Acylation of Nickel *meso*-Tetraarylporphyrins: Porphyrin to Corrole Ring Contraction and Formation of *seco*-Porphyrins

Christophe Jeandon, Romain Ruppert, and Henry J. Callot\*

UMR 7177 CNRS, Faculté de Chimie, Université Louis Pasteur, 1 rue Blaise Pascal, 67000 Strasbourg, France

callot@chimie.u-strasbg.fr

Received January 9, 2006



Friedel–Crafts acylation of nickel *meso*-tetraarylporphyrins with aryl anhydrides, followed by air oxidation in the presence of pyridine, DMAP, and excess anhydride, produced corroles in 8–21% yields. Other products include a porphyrinic ketone, an additional corrole whose bridge has been retained as an acyl group attached to a pyrrole, and a lactone resulting from the insertion of an oxygen atom into an  $\alpha,\beta$ -pyrrole bond. The ring contraction is best explained by a pinacolic rearrangement reminiscent of the one taking place in the formation of corrinoids, a benzyloxy group replacing the acetic side chain found in the natural products.

### Introduction

Aromatic electrophilic substitution at the pyrrolic positions of the porphyrin ring is an easy and useful method for functionalizing the macrocycle.<sup>1</sup> Among numerous examples, one can cite nitration, halogenation, and Vilsmeier–Haack formylation. However, the Friedel–Crafts acylation was almost limited to the alkylporphyrin series and several examples of acetylation of deuteroporphyrin derivatives or heptaethylporphyrin have been described.<sup>2</sup> To our knowledge, no example of a simple intermolecular acylation of a *meso*-tetraarylporphyrin was known when our work was initiated.

Our first results indicated that the outcome of this acylation reaction, although it was run under mild conditions, was dramatically influenced by the structure and the solubility of

the metalloporphyrin as well as the nature of the anhydride and that, under unfavorable conditions, low conversion and production of complex mixtures were the rule. We first demonstrated that acetylation of nickel *meso*-tetraarylporphyrins **1** gave porphyrin spiro dimers **2** in good yield (Scheme 1), that all steps leading to these compounds could be satisfactorily interpreted,<sup>3</sup> and that the peri interaction between a *meso*-aryl group and the acyl group was crucial.<sup>4</sup>

During this study, we also found that, under benzylation conditions, nickel *meso*-tetraarylporphyrins suffered a ring contraction to corroles **3** in yields up to 21%.<sup>5</sup> Corroles, like many unusual porphyrinoids showing expanded or contracted tetrapyrrolic macrocycles, have been intensively studied in the recent years with the development of new synthetic routes or the preparation of catalysts based on metallocorroles.<sup>6</sup>

(1) Vicente, M. G. H. in *The Porphyrin Handbook*; Kadish, K. M., Smith, K. M., Guillard, R., Eds.; Academic Press: Boston, MA, 2000; Vol. 1, pp 149–199. Jaquinod, L. in *The Porphyrin Handbook*; Kadish, K. M., Smith, K. M., Guillard, R., Eds.; Academic Press: Boston, MA, 2000; Vol. 1, pp 201–237.

(2) Brockmann, H., Jr.; Bliesener, K.-M.; Inhoffen, H. H. *Liebigs Ann. Chem.* **1968**, *718*, 148–161. Jeandon, C.; Bauder, C.; Callot, H. J. *Energy Fuels*, **1990**, *4*, 665–667. Clezy, P. S.; Prashar, J. K. *Aust. J. Chem.* **1990**, *43*, 825–837. Clezy, P. S.; Jenie, U.; Prashar, J. K. *Aust. J. Chem.* **1990**, *43*, 839–856. Xu, Y.; Jaquinod, L.; Wickramasinghe, A.; Smith, K. M. *Tetrahedron Lett.* **2003**, *44*, 7753–7756.

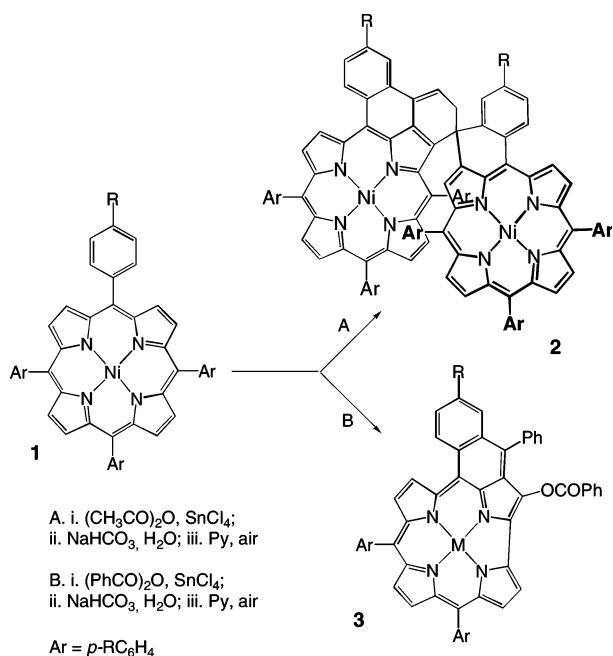
(3) Jeandon, C.; Ruppert, R.; Richeter, S.; Callot, H. J. *Org. Lett.* **2003**, *5*, 1487–1489.

(4) For a more general treatment of this peri reactivity of *meso*-tetraarylporphyrins, see: Callot, H. J.; Ruppert, R.; Jeandon, C.; Richeter, S. *J. Porphyrins Phthalocyanines* **2004**, *8*, 111–119.

(5) Jeandon, C.; Ruppert, R.; Callot, H. J. *Chem. Commun.* **2004**, 1090–1091.

(6) Gryko, D. T. *Eur. J. Org. Chem.* **2002**, 1735–1743. Ghosh, A. *Angew. Chem., Int. Ed.* **2004**, *43*, 1918–1931. Gryko, D. T.; Fox, J. P.; Goldberg, D. P. *J. Porphyrins Phthalocyanines* **2004**, *8*, 1091–1105.

## SCHEME 1



In this article, we will present the scope of this reaction, significant improvements of the reaction conditions, an analysis of the reaction sequence leading to the corroles helped by the isolation of two significant side products, and, for the crucial ring-contraction step, a mechanistic proposal that parallels the ring contraction involved in the biosynthesis of natural corrins. In addition, we present the characterization of lactonic *seco*-porphyrins obtained in parallel to the corroles.

## Results and Discussion

**Initial Results.** The benzylation of nickel *meso*-tetra-*p*-*t*-butyl- or *p*-ethoxy porphyrins, **4** and **5**, respectively, under conditions similar to that of the acetylation,<sup>3</sup> first produced a dark brown solution which was hydrolyzed to a green solution. While we studied the acetylation reaction, we found that addition of pyridine was crucial for the oxidative last step leading to the

## SCHEME 2

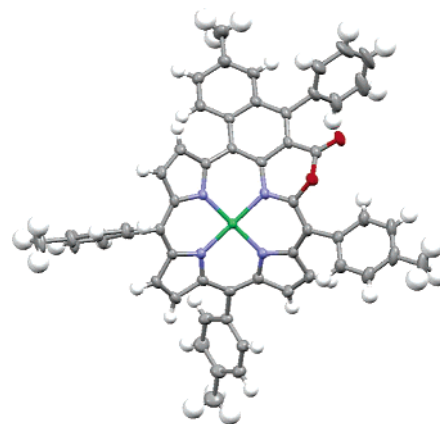
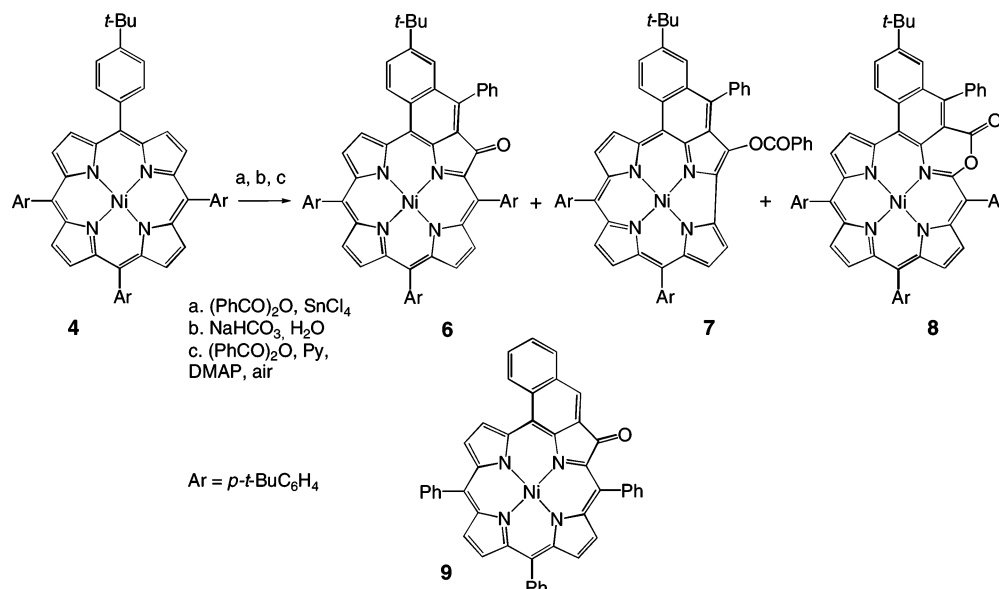


FIGURE 1. X-ray structure of lactone **10** (*p*-tolyl series).

spiro dimers.<sup>3</sup> Accordingly, when we used benzoic anhydride as the acylating agent and ran the reaction under similar conditions, the crude green hydrolysis solution was stirred in pyridine under air. Apart from polar untractable mixtures, three products of low polarity, **6**, **7**, and **8**, were isolated (Scheme 2; *p*-*t*-butyl series illustrated).

The major product was identified as ketone **6** (up to 35%, depending on the conditions). Its structure was easily deduced from its UV–visible and NMR spectra by comparison with the known ketone **9**.<sup>7</sup>

A minor and more polar porphyrinic product **8** was found in all reaction mixtures in less than 10% yield. Its spectral data (NMR and UV–visible) showed similarities with those of ketone **6**, but mass spectrometry revealed that one additional oxygen had been incorporated. An X-ray diffraction study showed that **8** was a lactone formed by insertion of an oxygen atom into an  $\alpha,\beta$  bond of the acylated pyrrole. Such an insertion was not known, although oxahomoporphyrins resulting from the cleavage of a  $\beta,\beta$  C–C bond and an oxygen insertion have been described.<sup>8</sup> In the *p*-tolyl series, a structure (Figure 1) could be obtained by X-ray diffraction and showed a highly ruffled *seco*-porphyrin ring. The lactonic ring has a flattened boat shape.

The presence of a blue-gray non-porphyrinic compound **7** of low polarity was unexpected. In the initial runs, the yields were

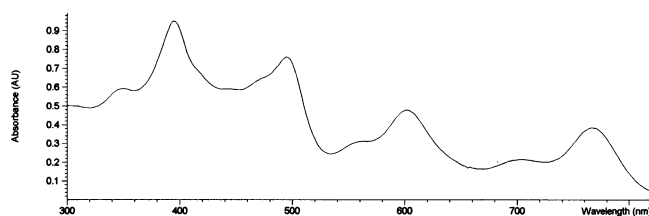


FIGURE 2. UV-visible spectrum of corrole 7.

very low (<5%). The NMR spectrum of **7** showed an absence of ring current, the signals for the pyrrole protons located between 5.7 and 7.2 ppm, the presence of only three *meso*-aryl groups, and an additional benzoyloxy group. Full assignment of the NMR signals was obtained for corrole **11**, produced by reaction of porphyrin **4** with *p*-methoxybenzoic anhydride. The UV-visible spectrum showed a multiband pattern unexpected for a porphyrin or an aromatic corrole (Figure 2).

Corrole **12** derived from the *p*-tolyl series gave crystals suitable for an X-ray diffraction study that confirmed the proposed ring contraction and the loss of a *meso* bridge (Figure 3). The macrocycle, including the nickel atom, is planar. For three pyrroles, the bond lengths are those expected for tetrapyrrolic macrocycles with  $C\beta-C\beta$  bonds shorter (observed 1.315–1.345 Å) than  $C\alpha-C\beta$  bonds (observed 1.415–1.443 Å). The two corresponding *meso* bridges also show the expected bond lengths. In the remaining pyrrole and the adjacent six-membered ring, there is evidence for alternating double and simple bonds with a cross-conjugated  $C\alpha-C\beta$  double bond: one  $C\alpha-C\beta$  bond and one C–C bond of the fused six-membered ring are short (respectively, 1.358 and 1.384 Å), whereas the other  $C\alpha-C\beta$  bond and the next C–C bond of the six-membered ring are among the longest of the benzomacrocycle (respectively, 1.445 and 1.446 Å). The nickel atom is square planar and bound to the N atoms through three long (1.881, 1.858, and 1.853 Å) and one shorter bond (1.806 Å) corresponding to the modified pyrrole. These distances are significantly shorter than those found in nickel porphyrins (ca 1.89–1.96 Å), whose ruffled geometry has often been correlated with the small size of the low-spin nickel(II).<sup>9</sup> The packing of the corrole molecules shows pairs of parallel and partially overlapping macrocycles, with the distance between the corrole planes averaging 3.7 Å.

**Scope of the Reaction and Optimization of the Corrole Yields.** A first drawback was clearly identified: the starting porphyrin had to be in solution before the reagents were added because all attempts to start the reaction under heterogeneous conditions failed. Low conversion and overreaction were observed.

In dichloromethane, the reaction was fast but the solubility of the porphyrin was the limiting factor. However, in the case

of the more soluble nickel *p*-alkoxyphenylporphyrins (ethoxy and longer chains) and by using a large excess of anhydride and  $\text{SnCl}_4$ , fair yields of corrole were obtained. In chloroform, the solubility increased but the reaction rate slowed significantly. Although the reaction was also slow at 20 °C in chlorobenzene, this solvent was selected in the case of nickel complexes of the poorly soluble *meso*-tetraphenylporphyrin and the *p*-alkylated analogues because it allowed the reaction mixture to be heated, up to more than 100 °C. Under these conditions, both the solubility and the reaction rate were satisfactory, but to avoid overreaction, the amount of anhydride had to be limited to a moderate excess. In polar solvents, such as nitromethane, the reaction was excessively slow and the conversion was negligible.

Under our conditions, substituted benzoic anhydrides bearing electron-withdrawing groups did not react, and one should remember that anhydrides derived from aliphatic carboxylic acid gave very different products, including porphyrin spiro dimers.<sup>3</sup>

The nature of the complexed metal was crucial: only nickel porphyrins gave corroles. When run under identical conditions, the corresponding palladium or copper complexes gave no detectable corrole derivatives but only porphyrinic products, as shown by their UV-visible spectra showing a high-intensity Soret band as well as several less-intense bands, typical for aromatic porphyrins or chlorins, and not the multiband (similar intensities) typical for the nonaromatic corroles.

The second step of the porphyrin to corrole conversion is an air oxidation of the crude product from the hydrolysis of the acylation mixture. This reaction was best run in pyridine, and we found that both an excess of anhydride and the addition of DMAP were beneficial. In the case of the acylations run in chlorobenzene with a slight excess of anhydride, addition of another anhydride led to corroles that had incorporated two different fragments: the additional carbon forming the six-membered ring and its aryl group from the first anhydride and then the ester from the second anhydride (Table 1).

In summary, the best corrole yields from nickel *meso*-tetraarylporphyrins were obtained in dichloromethane or chloroform in the presence of an excess of anhydride for the nickel alkoxyphenylporphyrins and in hot chlorobenzene with a moderate excess of anhydride for nickel alkylphenylporphyrins. In this last case, two different anhydrides may be used successively.

Finally, if one favors simplicity of the reaction conditions over yield, a one-pot procedure skipping the hydrolysis step may be followed. The crude acylation mixture can be evaporated to dryness and then treated with additional anhydride, pyridine, and DMAP. Yields of corroles up to 15% were obtained within a few hours. The results of various experiments are summarized in Table 1.

**Analysis of the Acylation/Cyclization Sequence.** In this and the two following sections, we will consider only products derived from porphyrin **4** (*p*-*t*-butyl series).

The first steps of the reaction sequence are easily drawn: acylation of a  $\beta$ -pyrrolic carbon followed by cyclization onto the neighboring aryl ring. However, the initial dark brown solution ( $\lambda_{\text{max}} = 406, 502, 726, 779, 860 \text{ nm}$ ; relative intensities = 1:0.65:0.32:0.32:0.33) was dramatically different from that of all classical porphyrin derivatives and strongly suggested that we observe cation **26** (charge arbitrarily located at the periphery of the rings; see Scheme 3). A similar cation was produced when hydroxyester **27**<sup>13</sup> was treated with acid ( $\lambda_{\text{max}} = 407, 499, 720, 792, 875 \text{ nm}$ ; relative intensities = 1:0.65:0.30:0.30:0.32). It is

(7) Ishkov, Y. V. *Russ. J. Org. Chem.* **2001**, *37*, 288–290. Richeter, S. Thèse de l'Université Louis Pasteur, Strasbourg, France, 2003. Richeter, S.; Jeandon, C.; Gisselbrecht, J.-P.; Graff, R.; Ruppert, R.; Callot, H. J. *Inorg. Chem.* **2004**, *43*, 251–263.

(8) Brückner, C.; Sternberg, E. D.; MacAlpine, J. K.; Rettig, S. J.; Dolphin, D. *J. Am. Chem. Soc.* **1999**, *121*, 2609–2610. Brückner, C.; Rettig, S. J.; Dolphin, D. *J. Org. Chem.* **1998**, *63*, 2094–2098. McCarthy, J. R.; Jenkins, H. A.; Brückner, C. *Org. Lett.* **2003**, *5*, 19–22.

(9) Sanders, J. K. M.; Bampos, N.; Clyde-Watson, Z.; Darling, S. L.; Hawley, J. C.; Kim, H.-J.; Mak, C. C.; Webb, S. J. in *The Porphyrin Handbook*; Kadish, K. M., Smith, K. M., Guillard, R., Eds.; Academic Press: Boston, MA, 2000; Vol. 3, pp 1–48. Scheidt, W. R. in *The Porphyrin Handbook*; Kadish, K. M., Smith, K. M., Guillard, R., Eds.; Academic Press: Boston, MA, 2000; Vol. 3, pp 49–112.

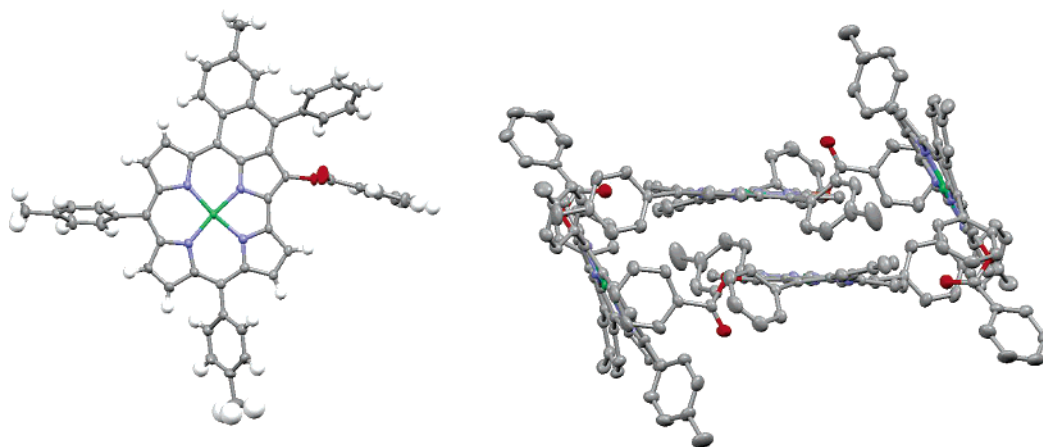
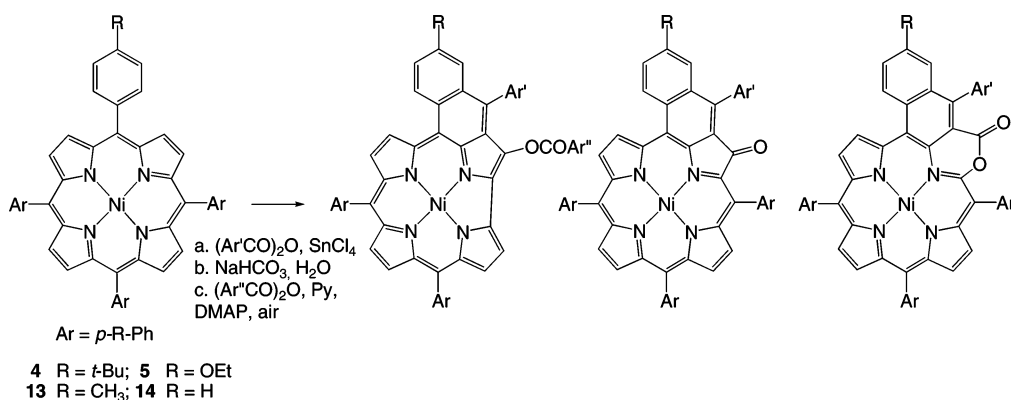


**FIGURE 3.** X-ray structure of corrole **12** (*p*-tolyl series). Single molecule viewed perpendicularly to the macrocycle ring and packing showing the parallel arrangement of molecule pairs (H omitted for clarity).

**TABLE 1.**



porphyrin	Ar'	Ar''	method <sup>a</sup>	% corrole, respective ketone, lactone
<b>4</b>	Ph	Ph	C	<b>7</b> (15); <b>6</b> (23); <b>8</b> (7)
<b>4</b>	<i>p</i> -MeOPh	Ph	C	<b>15</b> (17); <b>16</b> (28); <b>17</b> (9)
			D	<b>15</b> (13) <sup>b</sup>
<b>4</b>	<i>p</i> -MeOPh	<i>p</i> -MeOPh	C	<b>18</b> (20); <b>16</b> (24); <b>17</b> (3)
			C <sup>c</sup>	<b>18</b> (19) <sup>b</sup>
<b>5</b>	Ph	Ph	A	<b>19</b> (21); <b>20</b> (17); <b>21</b> (5)
			B	<b>19</b> (15) <sup>b</sup>
<b>5</b>	<i>p</i> -MeOPh	<i>p</i> -MeOPh	A	<b>22</b> (13) <sup>b</sup>
<b>13</b>	Ph	Ph	C	<b>12</b> (10); <b>23</b> (13); <b>10</b> (3)
<b>13</b>	<i>p</i> -MeOPh	Ph	C	<b>24</b> (12) <sup>b</sup>
<b>14</b>	<i>p</i> -MeOPh	Ph	C <sup>d</sup>	<b>25</b> (8) <sup>b</sup>

<sup>a</sup> Methods: see Experimental Section. <sup>b</sup> Only corrole collected. <sup>c</sup> Hydrolysis performed with water instead of saturated aqueous NaHCO<sub>3</sub>. <sup>d</sup> Reaction run at 115 °C; 15% starting material recovered.

also known that such extended porphyrinic cations show long wavelength absorptions.<sup>14</sup> When we treated alcohols **28** and **29** (see below) with acid (2% TsOH·H<sub>2</sub>O in CH<sub>2</sub>Cl<sub>2</sub>), a very similar (λ<sub>max</sub> within ± 2 nm) UV–visible spectrum was also observed.

(10) Miller, J. R.; Dorough, C. D. *J. Am. Chem. Soc.* **1952**, *74*, 3977–3981. Caughey, W. S.; Deal, R. M.; McLees, B. D.; Alben, J. O. *J. Am. Chem. Soc.* **1962**, *84*, 1735–1736. Cole, S. J.; Cuthoys, G. C.; Magnusson, E. A.; Phillips, J. N. *Inorg. Chem.* **1972**, *11*, 1024–1028.

(11) Callot, H. J.; Schaeffer, E.; Cromer, R.; Metz, F. *Tetrahedron* **1990**, *46*, 5253–5262.

(12) Golder, A. G.; Nolan, K. B.; Povey, D. C.; Milgrom, L. R. *J. Chem. Soc., Chem. Commun.* **1987**, 1788–1790.

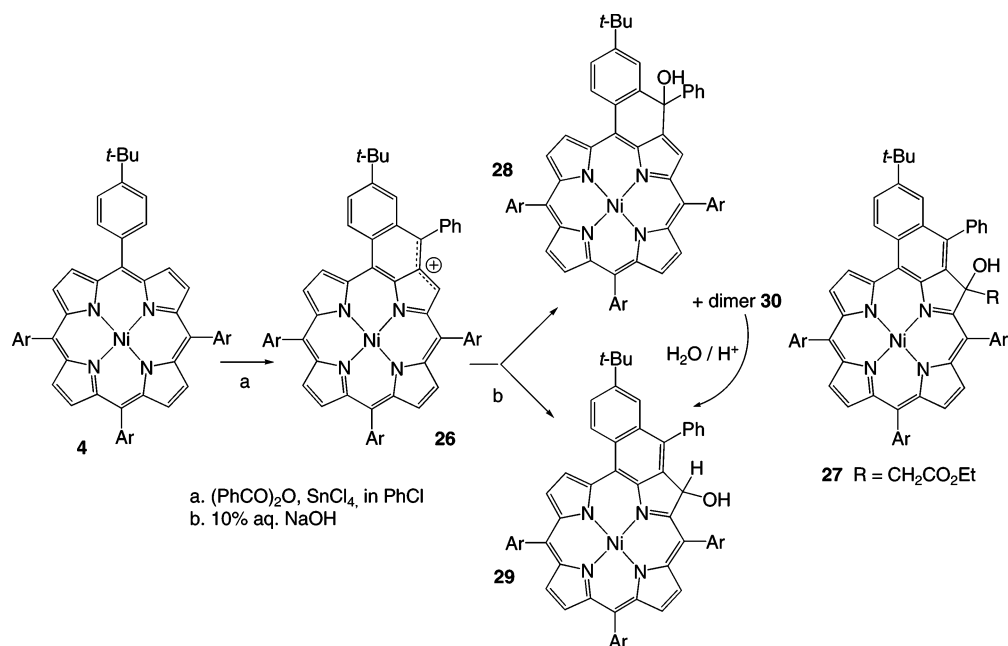
(13) Fouchet, J.; Jeandon, C.; Ruppert, R.; Callot, H. J. *Org. Lett.* **2005**, *7*, 5257–5260.

(14) Xu, Y.; Jaquinod, L.; Wickramasinghe, A.; Smith, K. M. *Tetrahedron Lett.* **2003**, *44*, 7753.

Hydrolysis of the postulated cationic intermediate **26** should lead to alcohols **28** and/or **29** or a corresponding tin derivative, depending on the basicity of the medium. Under our conditions (saturated aqueous sodium hydrogen carbonate), one would expect tin to remain bound and TLC analysis confirmed the high polarity of the product(s). In one run, we hydrolyzed the acylation mixture with water only with a negligible drop in yield (see Table 1).

Alternatively, alcohol **28** and its allylic isomer **29**, both of moderate polarity, were obtained when the solution was quenched with 10% aqueous sodium hydroxide. A third product **30** of very low polarity could be isolated in variable yield but never in a pure state. It is believed, from HRMS and NMR data (8 singlets corresponding to *tert*-butyl groups), to be an unsymmetrical dimeric ether. This absence of symmetry may

## SCHEME 3



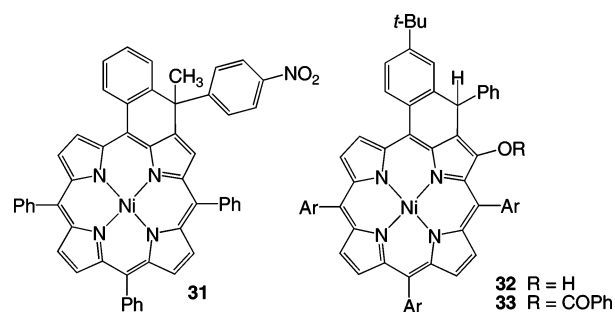
be due to either different connections (oxygen connected to a secondary or a tertiary carbon) or conformational restrictions imposing a gauche conformation. Upon attempted isolation, this dimer was cleaved to give alcohol **29**.

These experiments confirmed that the green hydrolysis solution obtained at low pH corresponded to a product that had not yet suffered ring contraction and that this product might be a tin derivative of alcohol **29** in agreement with the chlorin-like UV–visible spectrum of the solution ( $\lambda_{\text{max}} = 448, 618, 666 \text{ nm}$ ; relative intensities = 1.0:0.12:0.18). This partial hydrolysis was also crucial for obtaining the corrole because neither alcohol **28** nor alcohol **29** was a precursor of a corrole: when subjected to the ring contraction conditions, both were recovered unchanged. Only after a much longer reaction time did alcohol **29** slowly oxidize into ketone **6**.

**Ring Contraction: Mechanistic Hypotheses.** The ring contraction obviously involves several steps. Because the hydrolyzed acylation mixture is air stable in inert solvents, one has first to identify the factors triggering both the oxidation and the ring contraction of the substrate, then to put forward mechanistic hypotheses, and finally to try to isolate intermediates or significant byproducts or to synthesize independently hypothetical intermediates and follow their fate under the ring contraction conditions.

Nickel is a good candidate for triggering a ring contraction. The small nickel(II) cation does not fit into the porphyrin cavity<sup>9</sup> and thus induces deformations. On the contrary, the structure of corrole **7** shows a remarkable planarity and significantly shorter Ni–N bonds. Whatever the ring contraction substrate, its oxidation is dependent on the presence of pyridine. Such a pyridine-dependent oxidation was observed earlier, when we found that pyridine was crucial for the formation of spiro dimers upon acetylation/oxidation of nickel *meso*-tetraarylporphyrins. Only nickel may interfere with this potential ligand and, if mono- or bispyridine complexes<sup>10</sup> are formed and show more accessible redox potentials, this could explain the higher sensitivity of the porphyrin (the addition of DMAP should enhance this pyridine effect). On the other hand, coordination chemistry of square planar palladium porphyrins is unknown.<sup>9</sup> Evidence for such a

## SCHEME 4



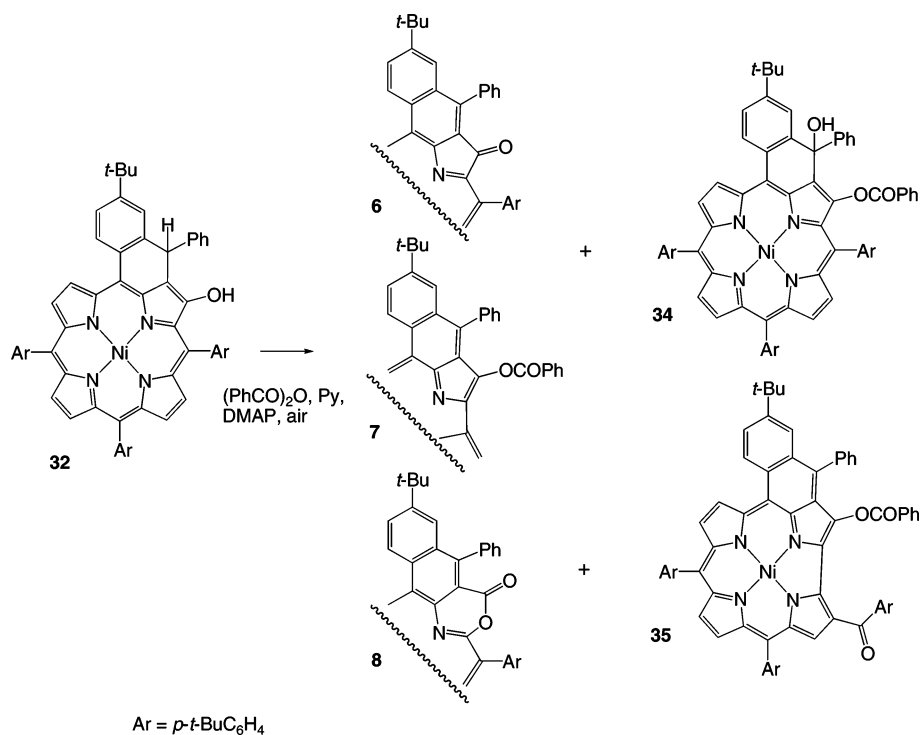
mechanism was found when we ran cyclic voltammetry experiments using porphyrin **31**<sup>11</sup> as a blocked model and found that indeed addition of 5% pyridine in a dichloroethane solution displaced the first oxidation wave of **31** by ca. 100 mV. In the case of palladium porphyrins, not only are the porphyrins less prone to oxidation<sup>12</sup> but also the axial coordination is inexistent.<sup>9</sup>

The higher yields observed under acylating conditions (excess anhydride, DMAP) suggested that benzylation of the pyrrolic  $\beta$ -position may “freeze” a hydroxyporphyrin such as **32** (*p*-*t*-butyl series and benzoic anhydride as the reagent selected for the following discussion), isomeric to alcohols **28** and **29**. Such a structure would incorporate an  $\text{sp}^3$  carbon bearing a triaryl-methylic C–H in the six-membered ring, a position obviously prone to easy oxidation, with any electron-deficient intermediate being stabilized by a porphyrin and two benzene rings. Compounds such as **32** and **33** (Scheme 4) may be intermediates, and we wished to synthesize them to realize a shortcut of the ring contraction sequence.

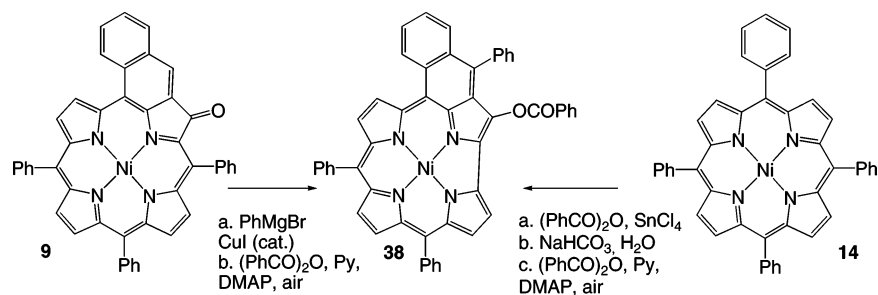
The obvious starting material was ketone **6**. Its preparation was independently optimized<sup>13</sup> up to 80% yield. After testing several reducing agents, we found that tetra-*n*-butylammonium borohydride<sup>15</sup> gave almost exclusively hydroxyporphyrin **32** (86%), which could be crystallized directly from the reaction

(15) D’Incan, E.; Loupy, A. *Tetrahedron* **1981**, *37*, 1171–1179.

## SCHEME 5



## SCHEME 6



mixture and proved to be moderately stable. Other reagents, such as sodium borohydride, yielded mixtures of **32**, chlorinic alcohol **29**, and blue tetrahydro derivatives that were not further investigated.

When subjected to the ring contraction conditions, **32** gave corrole **7** in a better yield (24%) than that of the direct reaction (15%), in addition to the usual byproducts, ketone **6** (27%) and lactone **8** (5%). Even more interesting was the isolation of a small amount of an oxidized porphyrin **34** (5%) and of an additional corrole **35** (4%) (Scheme 5).

The structure of hydroxybenzoate **34** was easily deduced from its UV–visible and NMR data, which were very similar to those of alcohol **28**, except for the absence of the pyrrolic singlet at 8.73 ppm and the presence of a singlet at 4.12 ppm due to the hydroxyl proton and the presence of the benzoate proton signals. In the case of corrole **35**, its UV–visible and mass spectrometric data, as well as the simultaneous presence of signals for all *tert*-butylphenyl groups, and a pyrrolic singlet strongly suggested the retention of the bridge as a *p*-*t*-butylbenzoyl moiety. NMR correlations and a preliminary X-ray diffraction study confirmed the proposed structure (*p*-tolyl series, see Supporting Information). After having isolated these two minor compounds starting with **33**, we went back to the initial reaction conditions and

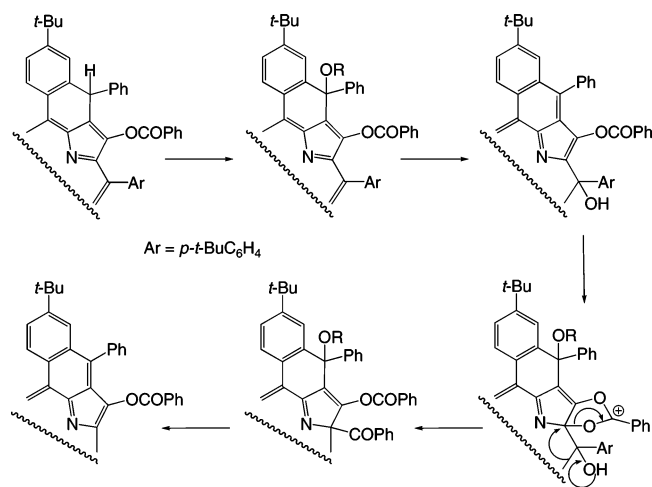
found that they were also present but difficult to detect in the more complex mixture resulting from the acylation.

The 1,4-reduction reaction was also run starting with **36**,<sup>13</sup> the palladium analogue of ketone **6**, and gave the corresponding hydroxyprophyrin **37** in good yield. However, when subjected to ring contraction conditions, this compound gave exclusively porphyrinic products, the major one being starting ketone **36**.

Finally, one should remember that, during the preliminary study<sup>5</sup> of the ring contraction, a hydroxyprophyrin (*meso*-tetraphenylporphyrin series) was produced via 1,4-addition of PhMgBr onto ketone **9** in the presence of CuI (Scheme 6). The resulting hydroxyprophyrin gave the corresponding corrole **38** in 10% yield. The same corrole could also be obtained in 6% yield using method A in chloroform.

Without the data presented above, the ring contraction mechanism would have been quite mysterious because the examples from the literature would have been of little help. A couple of porphyrin, porphyrin isomer, and porphyrin homologue or heteroanalogue (phthalocyanines and porphyrazines) ring contractions are known,<sup>16</sup> but the mechanistic discussion is often minimal. In our case, the ring contraction is clearly coupled with an oxidation process and, at variance with the other

SCHEME 7



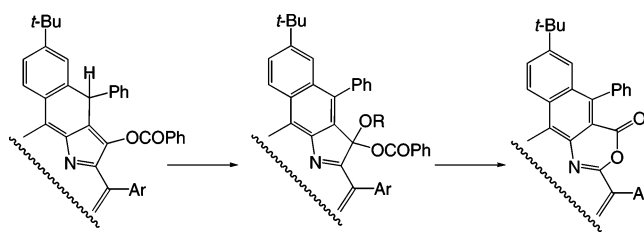
examples, may involve a neighboring group, the benzoate moiety.

The initial step (Scheme 7) could be the benzylation of the hydroxyporphyrin to freeze the hydroxyporphyrin structure, followed by the oxidation at the triphenylmethylic position, as hypothesized above. Compound **34** is a witness of this process. The oxygenated fragment (OR = OH, OCOPh, or peroxy analogues) may then leave this position as an anion with concomitant addition of a hydroxyl group onto the meso bridge, resulting in (a) the loss of aromaticity and an increase of reactivity of the conjugated system and (b) possibly a relief of stress by shortening the Ni–N bonds.

By analogy to the aerobic pathway leading to the framework of corrins,<sup>17</sup> we propose that the benzoate could act similarly to the acetic chain in the latter case and forms a cyclic ketal by addition to an oxidized species. The next step, a pinacol rearrangement, would parallel that observed in the natural series. Elimination of the benzoyl moiety as a benzoate anion may produce the major corrole. Alternatively, this benzoyl moiety may migrate first to the vicinal pyrrole  $\alpha$ -position to relieve steric strain and then to the  $\beta$ -pyrrolic position to achieve a better conjugation and thus give minor corroles **35**.

**Formation of Lactonic *seco*-Porphyrins.** The formation of ketone **6** is straightforward and could be optimized by addition of chloranil and acid to the hydrolysis product,<sup>13</sup> but that of lactone **8** is less clear. Under ring contraction conditions, ketone **6** did not produce lactone **8**. Because the structure of **8** suggested a Bayer–Villiger-type oxidation, we reacted ketone **6** with *m*-chloroperbenzoic acid. Even under very mild conditions (diluted solutions, slow addition), no lactone was observed and the reaction led to complete destruction of the porphyrin ring. We propose (Scheme 8) that lactone **8** forms via allylic isomers

SCHEME 8



of those leading to the corrole (R = OH, OCOPh, for example). An intermediate bearing two gem-oxygenated substituents, one of them at the peroxy oxidation level, may then suffer a rearrangement similar to the Bayer–Villiger one yielding lactone **8**. Looking back at the attempted Bayer–Villiger reaction on ketone **6**, the differences are clear: Ketone **6** has a low electrophilic reactivity, and competition with the oxidation of the conjugated system may be very unfavorable. On the other hand, an intermediate such as the one proposed has all the appropriate functional groups already positioned for the ring enlargement to the lactone.

## Conclusion

The results described in this work underline an apparent paradox: starting with porphyrins known for their stability and complexing an usually inert metal, and by running a classical organic reaction, a highly unexpected reaction sequence operated and gave new corroles. The paradox is however only apparent because: (a) all substituents (including hydrogen) of tetraarylporphyrins are arranged in a peri geometry; (b) interactions between these substituents will favor reactions between neighboring groups; (c) flattening of the conjugated system, in particular if one considers the *meso*-aryl proton/pyrrole proton distances, will increase strain; (d) nickel will favor any reaction resulting in folding or ring contraction that will shorten metal–nitrogen bonds; (e) if one suspects a mechanism similar to that leading to corrins, a neighboring group (benzoate) is ideally placed for triggering the ring contraction. As in the case of acetylation that gave new spiro bisporphyrins, the corresponding benzylation results in the serendipitous production of a new series of nonaromatic divalent corroles, whose study should now be developed.

## Experimental Section

**Preparation of Corroles from Nickel *meso*-Tetraarylporphyrins.** The following experimental procedures all yield corroles, ketones, and lactones, as well as several minor products. Because the aim of the study was the optimization of the corrole yields as well as the search for the mechanism of its formation, the other components were only isolated in selected cases (see Table 1).

**Method A** (two steps, large excess anhydride, low or high temperature). The nickel porphyrin (0.05 mmol) and the anhydride (1.0 mmol) were dissolved in CHCl<sub>3</sub> (15 mL; distilled from P<sub>2</sub>O<sub>5</sub>), and SnCl<sub>4</sub> (0.4 mL) was added at once. The flask solution was stirred until full conversion of the starting material (ca. 3 days at +20 °C or 10 h under reflux). The solution was diluted with CH<sub>2</sub>-Cl<sub>2</sub> (25 mL), poured into a large excess of aqueous NaHCO<sub>3</sub>, and stirred for 30 min (the color changed from brown to green) and then decanted and washed three times with water, dried over Na<sub>2</sub>SO<sub>4</sub>, and evaporated. To the green residue in a 25 mL round-bottomed flask was added (dimethylamino)pyridine (0.82 mmol), benzoic anhydride (0.16 mmol), and pyridine (10 mL). The resulting solution was stirred under a dry-air atmosphere for 4 h. Pyridine

(16) Tse, M. K.; Zhang, Z.; Mak, T. C. W.; Chan, K. S. *Chem. Commun.* **1998**, 1199–1200. Will, S.; Rahbar, A.; Schmickler, H.; Lex, J.; Vogel, E. *Angew. Chem., Int. Ed.* **1990**, *29*, 1390–1393. Neumann, K. L. Ph.D. Dissertation, University of Cologne, Germany, 1994; p 37. Callot, H. J.; Rohrer, A.; Tschamber, T. *New J. Chem.* **1995**, *19*, 155–159. Callot, H. J.; Schaeffer, E. *J. Chem. Res. (S)* **1978**, 51; (M) **1978**, 690–697. Li, J.; Subramanian, L. R.; Hanack, M. *Eur. J. Org. Chem.* **1998**, 2759–2767. Fujiki, M.; Tabei, H.; Isa, K. *J. Am. Chem. Soc.* **1986**, *108*, 1532–1536. Ramdhanie, B.; Stern, C. L.; Goldberg, D. P. *J. Am. Chem. Soc.* **2001**, *123*, 9447–9448. Kobayashi, N.; Yokoyama, M.; Muranaka, A.; Ceulemans, A. *Tetrahedron Lett.* **2004**, *45*, 1755–1758. Vogel, E.; Michels, M.; Zander, L.; Lex, J.; Tuzun, N. S.; Houk, K. N. *Angew. Chem., Int. Ed.* **2003**, *42*, 2857.

(17) Battersby, A. R. *Nat. Prod. Rep.* **2000**, *17*, 507–526.

was evaporated under reduced pressure, and then toluene (3 × 10 mL) was added and evaporated under vacuum to eliminate the last traces of pyridine. The residue was chromatographed (silica gel; 100 mL, toluene in the case of nickel *meso*-tetraalkoxy porphyrins). Elution with the same solvent gave the corrole after crystallization from CH<sub>2</sub>Cl<sub>2</sub>–MeOH. The corresponding ketone and lactone were then eluted and crystallized from CH<sub>2</sub>Cl<sub>2</sub>–MeOH.

Depending on the substitution of the porphyrin and the anhydride, minor adjustments of the chromatographic procedure were necessary. In the case of alkyl-substituted tetraarylporphyrins, the products were eluted using a solvent gradient from cyclohexane + toluene 1:1 to pure toluene. Use of methoxylated anhydrides may change the elution order.

**Method B** (one pot, large excess of anhydride, low temperature). The same acylation procedure as that in method A was followed, but the hydrolysis step was not performed and the crude brown solution evaporated under reduced pressure. The residue was treated as above with benzoic anhydride and (dimethylamino)pyridine in pyridine, but the highest yield of corrole **7** (15%; isolation procedure as above) was obtained after a longer reaction time (16 h).

**Method C** (two steps, moderate excess of a first anhydride, high temperature; second step run with the same or a different anhydride). A nickel tetraarylporphyrin (0.12 mmol) in chlorobenzene (10 mL) was heated to 75–80 °C and stirred until it was dissolved. To this solution was added SnCl<sub>4</sub> (0.3 mL), followed by the solid anhydride (0.25 mmol). The reaction was followed by TLC. After 0.5 h (and again after 1.0 h if there remained some starting material), anhydride was added in 0.25 mmol portions. After full conversion of the starting material (ca. 2 h), the hydrolysis of the solution and the second step were performed as in method A. However, if one wishes to introduce a different carboxylate moiety, the second step may be run using another anhydride in large excess (1.0 mmol) to avoid any interference with some remaining first anhydride.

In one example, the crude acylation solution was not neutralized with saturated aqueous NaHCO<sub>3</sub> but was washed six times with water (200 mL). Under these conditions, corrole **18** was obtained in 19% yield.

**Method D** (one pot, slight excess of anhydride, high temperature). The same acylation procedure as that in method C was followed, but the hydrolysis step was not performed and the crude brown solution evaporated under reduced pressure. The second step was run as in method C.

**Corrole 7.** <sup>1</sup>H NMR (CDCl<sub>3</sub>): δ = 7.59 (d, 1H, *J* = 9 Hz, cyclized phenyl), 7.53 (broad d, 2H, *J* = ca. 7.5 Hz, benzoate *o*-H), 7.50 (tt, 1H, *J* = 7.5 and ca. 1 Hz, benzoate *p*-H), 7.38 (d, 2H, *J* = 7.8 Hz, *tert*-butylphenyl AB), 7.35 (d, 2H, *J* = 7.8 Hz, *tert*-butylphenyl), 7.2–7.3 (m, 9H, 4 *tert*-butylphenyl + 2 benzoate *m*-H + 2 phenyl on six-membered ring *o*-H + 1 pyrrole), 7.12 (t, 2H, *J* = 7.5 Hz, phenyl on six-membered ring *m*-H), 7.05 (dd, 1H, *J* = 9 and 2.1 Hz, cyclized phenyl), 6.98 (tt, 1H, *J* = 7.5 and ca. 1 Hz, phenyl on six-membered ring *p*-H), 6.78 (d, 1H, *J* = 2.1 Hz, cyclized phenyl), 6.66, 6.18, 6.02, 5.93, 5.81 (5d, 5 × 1H, *J* = respectively, 5.1, 4.8, 4.5, 4.8, 4.5 Hz, pyrrole), 1.36, 1.32, 1.07 (3s, 9 + 9 + 9H, *tert*-butyl). UV–visible (CH<sub>2</sub>Cl<sub>2</sub>): λ = 388 nm (ε = 74 000), 450 (51 000), 488 (43 500), 600 (31 500), 694 (16 600), 760 (24 800). HRMS: calcd for C<sub>63</sub>H<sub>54</sub>N<sub>4</sub>O<sub>2</sub>Ni+H<sup>+</sup>, 957.3660; found, 957.3658.

**Ketone 6.** <sup>1</sup>H NMR (CDCl<sub>3</sub>): δ = 8.91 and 8.55 (2d, 1 + 1H, *J* = 5.1 Hz, pyrrole), 8.17 and 7.89 (2d, 1 + 1H, *J* = 5.1 Hz, pyrrole), 8.11 and 8.03 (2d, 1 + 1H, *J* = 4.8 Hz, pyrrole), 8.39 (d, 1H, *J* = 7.5 Hz, cyclized phenyl), 7.85 (dd, 1H, *J* = 7.5 and 2 Hz, cyclized phenyl), 7.85–7.45 (m, 18H, 12 *tert*-butylphenyl + 1H of cyclized phenyl + 5 phenyl on six-membered ring), 1.52, 1.49, 1.43, 1.33 (4s, 9 + 9 + 9 + 9H, *tert*-butyl). UV–visible (CH<sub>2</sub>Cl<sub>2</sub>): λ<sub>max</sub> = 414 nm (ε = 73 000), 466 (35 000), 494 (36 000), 714 (20 000). HRMS: calcd for C<sub>67</sub>H<sub>62</sub>N<sub>4</sub>ONi+H<sup>+</sup>, 997.4350; found, 997.4350.

**Lactone 8.** <sup>1</sup>H NMR (CDCl<sub>3</sub>): δ = 8.47, 8.24, 8.06, 7.93, 7.74 (5d, 1 + 1 + 1 + 1 + 1H, *J* = respectively, 4.5, 4.5, 5.1, 4.8, 4.8

Hz, pyrrole), 8.04 (d, 1H, *J* = 8.7 Hz, cyclized phenyl), 7.80 (dd, 1H, *J* = 8.7 and 1.8 Hz, cyclized phenyl), 7.4–7.8 (m, 19H, 12 *tert*-butylphenyl + 1 cyclized phenyl + 1 pyrrole + 5 phenyl on six-membered ring), 1.50, 1.46, 1.40, 1.27 (4s, 9 + 9 + 9 + 9H, *tert*-butyl). UV–visible (CH<sub>2</sub>Cl<sub>2</sub>): λ = 420 nm (sh., ε = ca. 50 000), 454 (91 000), 630 (sh., ca. 6300), 672 (20 400). HRMS: calcd for C<sub>67</sub>H<sub>62</sub>N<sub>4</sub>O<sub>2</sub>Ni+H<sup>+</sup>, 1013.4299; found, 1013.4255.

**Corrole 15.** <sup>1</sup>H NMR (CDCl<sub>3</sub>): δ = 7.62 (d, 2H, *J* = 7.5 Hz, benzoate *o*-H), 7.60 (d, 1H, *J* = 9 Hz, cyclized phenyl), 7.53 (broad t, 1H, *J* = ca. 7.5 Hz, benzoate *p*-H), 7.25–7.4 (m, 11H, 8 *tert*-butylphenyl + 2 benzoate *m*-H + 1 pyrrole), 7.18 and 6.60 (2d, AB, 4H, *J* = 8 Hz, *p*-methoxyphenyl), 7.05 (dd, 1H, *J* = 9 and 2.4 Hz, cyclized phenyl), 6.90 (d, 1H, *J* = 2.4 Hz, cyclized phenyl), 6.68, 6.20, 6.04, 5.96, 5.85 (5d, 1 + 1 + 1 + 1 + 1H, *J* = respectively, 5.0, 4.5, 4.5, 5.0, 4.5 Hz, pyrrole), 3.45 (s, 3H, methoxy), 1.36, 1.32, 1.09 (3s, 9 + 9 + 9H, *tert*-butyl). UV–visible (CH<sub>2</sub>Cl<sub>2</sub>): λ = 388 nm (ε = 56 000), 466 (30 500), 490 (32 400), 604 (23 300), 698 (11 500), 758 (20 200). HRMS: calcd for C<sub>64</sub>H<sub>56</sub>N<sub>4</sub>O<sub>3</sub>Ni+H<sup>+</sup>, 987.3779; found, 987.3811.

**Ketone 16.** <sup>1</sup>H NMR (CDCl<sub>3</sub>): δ = 8.91, 8.55 (2d, 1 + 1H, *J* = respectively, 5.1, 4.8 Hz, pyrrole), 8.38 (d, 1H, *J* = 8.7 Hz, cyclized phenyl), 8.17, 8.12, 8.03 (3d, 1 + 1 + 1H, *J* = respectively, 5.1, 4.8, 4.8 Hz, pyrrole), 7.94 (d, 1H, *J* = 1.8 Hz, cyclized phenyl), 7.91 (d, 1H, *J* = 5.1 Hz, pyrrole), 7.85 (dd, 1H, *J* = 8.7 and 1.8 Hz, cyclized phenyl), 7.84–7.43 (m, 14H, 12 *tert*-butylphenyl + 2 *p*-methoxyphenyl), 7.13 (d, 2H, *J* = 8.7 Hz, *p*-methoxyphenyl), 3.95 (s, 3H, methoxy), 1.53, 1.49, 1.47, 1.36 (4s, 9 + 9 + 9 + 9H, *tert*-butyl). UV–visible (CH<sub>2</sub>Cl<sub>2</sub>): λ = 418 nm (ε = 83 500), 466 (40 500), 496 (41 200), 710 (22 400). HRMS: calcd for C<sub>68</sub>H<sub>64</sub>N<sub>4</sub>O<sub>2</sub>Ni+H<sup>+</sup>, 1027.4456; found, 1027.4435.

**Lactone 17.** <sup>1</sup>H NMR (CDCl<sub>3</sub>): δ = 8.47, 8.24, 8.05 (3d, 1 + 1 + 1H, *J* = 4.8, 4.8, 5.1 Hz, pyrrole), 8.03 (d, 1H, *J* = 8.5 Hz, cyclized phenyl), 7.92 (d, 1H, *J* = 5.1 Hz, pyrrole), 7.80 (dd, 1H, *J* = 8.5 and 2.5 Hz, cyclized phenyl), 7.75 (d, 1H, *J* = 2.5 Hz, cyclized phenyl), 7.74 (d, 1H, *J* = 4.8 Hz, pyrrole), ca. 7.8 (broad signal) and 7.65–7.5 (broad m, total 15H, 12 *tert*-butylphenyl + 2 *p*-methoxyphenyl + 1 pyrrole), 7.20 and 7.18 (2dd, AB, 1 + 1H, *J* = ca. 7 and 2 Hz, 2 *p*-methoxyphenyl), 4.0 (s, 3H, methoxy), 1.53, 1.46, 1.41, 1.30 (4s, 9 + 9 + 9 + 9H, *tert*-butyl). UV–visible (CH<sub>2</sub>Cl<sub>2</sub>): λ = 460 nm (ε = 85 000), 656 (15 300), 692 (20 700). HRMS: calcd for C<sub>68</sub>H<sub>64</sub>N<sub>4</sub>O<sub>3</sub>Ni+H<sup>+</sup>, 1043.4405; found, 1043.4421.

**Corrole 18.** <sup>1</sup>H NMR (CDCl<sub>3</sub>): δ = 7.59 (d, 1H, *J* = 8.5 Hz, cyclized phenyl), 7.55 (d, 2H, *J* = 8.5 Hz, benzoate *o*-H), 7.38, 7.34, 7.25, 7.24 (4d, 2 + 2 + 2 + 2H, *J* = 8.2 Hz, 8 *tert*-butylphenyl), 7.25 (d, 1H, *J* = 5.0 Hz, pyrrole), 7.13 (d, 2H, *J* = 9 Hz, *p*-methoxyphenyl), 7.04 (dd, 1H, *J* = 8.5 and 2.5 Hz, cyclized phenyl), 6.88 (d, 1H, *J* = 2.5 Hz, cyclized phenyl), 6.79 (d, 2H, *J* = 8.5 Hz, benzoate), 6.68 (d, 1H, *J* = 5.0 Hz, pyrrole), 6.62 (d, 2H, *J* = 9 Hz, *p*-methoxyphenyl), 6.20, 6.05, 5.96, 5.87 (4d, 1 + 1 + 1 + 1H, *J* = respectively, 4.5, 4.5, 5.0, 4.5 Hz, pyrrole), 3.86, 3.50 (2s, 3 + 3H, methoxy), 1.37, 1.32, 1.09 (3s, 9 + 9 + 9H, *tert*-butyl). UV–visible (CH<sub>2</sub>Cl<sub>2</sub>): λ = 388 nm (ε = 61 000), 464 (33 100), 490 (35 500), 602 (25 200), 698 (12 600), 760 (22 600). HRMS: calcd for C<sub>65</sub>H<sub>58</sub>N<sub>4</sub>O<sub>4</sub>Ni+H<sup>+</sup>, 1017.3884; found, 1017.3919.

**Corrole 19.** <sup>1</sup>H NMR (CDCl<sub>3</sub>): δ = 7.54 (d, 1H, *J* = 9 Hz, cyclized phenyl), 7.51 (d, 2H, *J* = 8.4 Hz, phenyl), 7.48 (d, 1H, *J* = 8.4 Hz, phenyl), 7.18–7.30 (m, 11H, 10 phenyl and ethoxyphenyl, 1 pyrrole H), 6.93 (t, 1H, *J* = 7.5 Hz, phenyl *para*-H), 6.88 and 6.83 (2d, 2 + 2H, *J* = 9 Hz, ethoxyphenyl), 6.62 (dd, 1H, *J* = 3 and 9 Hz, cyclized phenyl), 6.58 (d, 1H, *J* = 5.1 Hz, pyrrole), 6.19 (d, 1H, *J* = 3 Hz, cyclized phenyl), 6.10 (d, 1H, *J* = 4.8 Hz, pyrrole), 5.91 (d, 1H, *J* = 4.5 Hz, pyrrole), 5.87 (d, 1H, *J* = 4.5 Hz, pyrrole), 5.72 (d, 1H, *J* = 4.8 Hz, pyrrole), 4.07, 4.03 and 3.68 (3q, 2 + 2 + 2H, *J* = 7 Hz, ethoxy CH<sub>2</sub>), 1.44, 1.41 and 1.22 (3t, 3 + 3 + 3H, *J* = 7 Hz, ethoxy CH<sub>3</sub>). UV–visible (CH<sub>2</sub>Cl<sub>2</sub>): λ = 394 nm (ε = 53 000), 494 (43 000), 555 (sh., 18 000), 600 (28 000), 702 (12 600), 766 (22 000).



**Ketone 20.**<sup>5</sup> <sup>1</sup>H NMR (CDCl<sub>3</sub>):  $\delta$  = 8.84 (d, 1H,  $J$  = 4.5 Hz, pyrrole), 8.52 (d, 1H,  $J$  = 4.5 Hz, pyrrole), 8.38 (d, 1H,  $J$  = 9.3 Hz, cyclized phenyl), 8.16 (d, 1H,  $J$  = 5.2 Hz, pyrrole), 8.10 (d, 1H,  $J$  = 5.2 Hz, pyrrole), 8.02 (d, 1H,  $J$  = 4.8 Hz, pyrrole), 7.93 (d, 1H,  $J$  = 4.8 Hz, pyrrole), 7.79, 7.71, 7.40, 7.17, 7.11, 7.00 (6d, 2 + 2 + 2 + 2 + 2H,  $J$  = 9 Hz, *p*-ethoxyphenyl), 7.5–7.6 (m, 5H, phenyl), 7.41 (dd, 1H,  $J$  = 9.3 and 3 Hz, cyclized phenyl), 7.24 (d, 1H,  $J$  = 3 Hz, cyclized phenyl), 4.25, 4.22, 4.14, 4.02 (4q, 2 + 2 + 2 + 2H,  $J$  = 7 Hz, ethoxy CH<sub>2</sub>), 1.56, 1.53, 1.48, 1.41 (4t, 3 + 3 + 3 + 3H,  $J$  = 7 Hz, ethoxy CH<sub>3</sub>). UV–visible (CH<sub>2</sub>Cl<sub>2</sub>):  $\lambda$  = 420 nm ( $\epsilon$  = 101 000), 472 (41 000), 500 (36 000), 680 (sh., 14 000), 722 (27 000).

**Lactone 21.** <sup>1</sup>H NMR (45 °C, CDCl<sub>3</sub>):  $\delta$  = 8.39, 8.23 (2d, 1 + 1H,  $J$  = 4.8 Hz, pyrrole), 8.03 (d, 1H,  $J$  = 9 Hz, cyclized phenyl), 8.01, 7.90 (2d, 1 + 1H,  $J$  = respectively, 5.1, 4.8 Hz, pyrrole), 7.77 (d, 2H,  $J$  = 8.7 Hz, aryl), 7.74 (d, 1H,  $J$  = 4.8 Hz, pyrrole), 7.65–7.55 (m, 7H, aryl), 7.55 (d, 1H,  $J$  = 5.1 Hz, pyrrole), 7.50 (broad d, 2H,  $J$  = ca. 8.5 Hz, aryl), 7.37 (dd, 1H,  $J$  = 9 and 2.7 Hz, cyclized phenyl), 7.14, 7.07 (2d, 2 + 2H,  $J$  = 8.7 Hz, aryl), 7.04 (d, 1H,  $J$  = 2.7 Hz, cyclized phenyl), 7.02 (d, 2H,  $J$  = 9 Hz, aryl), 4.22, 4.19, 4.13 (3q, 2 + 2 + 2H,  $J$  = 7 Hz, ethoxy CH<sub>2</sub>), 3.94 (m, 2H, ethoxy CH<sub>2</sub>), 1.54, 1.51, 1.49, 1.37 (4t, 3 + 3 + 3 + 3H,  $J$  = 7 Hz, ethoxy CH<sub>3</sub>). UV–visible (CH<sub>2</sub>Cl<sub>2</sub>):  $\lambda$  = 420 nm ( $\epsilon$  = 44 500), 470 (96 500), 688 (27 300). HRMS: calcd for C<sub>59</sub>H<sub>46</sub>N<sub>4</sub>O<sub>6</sub>Ni+H<sup>+</sup>, 965.2844; found, 965.2838.

**Corrole 22.** <sup>1</sup>H NMR (CDCl<sub>3</sub>):  $\delta$  = 7.56 (d, 1H,  $J$  = 9 Hz, cyclized phenyl), 7.53 (d, 2H,  $J$  = 8.7 Hz, aryl), 7.22–7.16 (m, 5H, 4 aryl + 1 pyrrole), 7.11, 6.89, 6.83, 6.79 (4d, 2 + 2 + 2 + 2H,  $J$  = 9 Hz, aryl), 6.63 (dd, 1H,  $J$  = 9 and 2.4 Hz, cyclized phenyl), 6.62 (d, 1H,  $J$  = 5 Hz, pyrrole), 6.61 (d, 2H,  $J$  = 9 Hz, aryl), 6.30 (d, 1H,  $J$  = 2.4 Hz, cyclized phenyl), 6.14, 5.97, 5.91, 5.80 (4d, 1 + 1 + 1 + 1H,  $J$  = 4.5 Hz, pyrrole), 4.06, 4.05, 3.71 (3q, 2 + 2 + 2H,  $J$  = 7 Hz, ethoxy CH<sub>2</sub>), 3.85, 3.49 (2s, 3 + 3H, methoxy), 1.45, 1.41, 1.24 (3t, 3 + 3 + 3H,  $J$  = 7 Hz, ethoxy CH<sub>3</sub>). UV–visible (CH<sub>2</sub>Cl<sub>2</sub>):  $\lambda$  = 394 nm ( $\epsilon$  = 50 500), 475 (sh., 33 000), 492 (33 600), 604 (19 800), 698 (10 800), 766 (16 500). HRMS: calcd for C<sub>59</sub>H<sub>46</sub>N<sub>4</sub>O<sub>7</sub>Ni+H<sup>+</sup>, 981.2793; found, 981.2793.

**Corrole 12.** <sup>1</sup>H NMR (CDCl<sub>3</sub>):  $\delta$  = 7.58–7.46 (m, 4H, 1 cyclized phenyl, benzoate *o*- and *p*-H), 7.32–7.12 (m, 15H, 14 aryl + 1 pyrrole), 6.95 (broad t, 1H,  $J$  = 7.5 Hz, phenyl on six-membered ring *p*-H), 6.81 (dd, 1H,  $J$  = 8.4 and 1.8 Hz, cyclized phenyl), 6.63 (d, 1H,  $J$  = 5.7 Hz, pyrrole), 6.56 (broad s, 1H, cyclized phenyl), 6.13, 5.97, 5.92, 5.79 (4d, 1 + 1 + 1 + 1H,  $J$  = respectively, 4.5 Hz, pyrrole), 2.40, 2.36, 2.02 (3s, 3 + 3 + 3H, methyl). UV–visible (CH<sub>2</sub>Cl<sub>2</sub>):  $\lambda$  = 388 nm ( $\epsilon$  = 59 000), 466 (32 500), 488 (34 000), 598 (23 700), 698 (11 400), 762 (19 600). HRMS: calcd for C<sub>54</sub>H<sub>36</sub>N<sub>4</sub>O<sub>2</sub>Ni+H<sup>+</sup>, 831.2265; found, 831.2249.

**Ketone 23.** <sup>1</sup>H NMR (CDCl<sub>3</sub>):  $\delta$  = 8.88, 8.51, 8.15, 8.08, 8.00, 7.92 (6d, 1 + 1 + 1 + 1 + 1 + 1H,  $J$  = respectively, 4.8, 4.8, 5.1, 4.8, 4.8, 5.1 Hz, pyrrole), 8.35 (d, 1H,  $J$  = 8.4 Hz, cyclized phenyl), 7.75–7.55, 7.5–7.35 (2m, 17H, 2 cyclized phenyl + 15 aryl), 7.28 (d, 2H,  $J$  = 8.7 Hz, aryl), 2.60, 2.56, 2.48, 2.46 (4t, 3 + 3 + 3 + 3H, methyl). UV–visible (CH<sub>2</sub>Cl<sub>2</sub>):  $\lambda$  = 414 nm ( $\epsilon$  = 91 000), 466 (43 200), 494 (44 200), 714 (25 100). HRMS: calcd for C<sub>55</sub>H<sub>38</sub>N<sub>4</sub>ONi+H<sup>+</sup>, 829.2472; found, 829.2466.

**Lactone 10.** <sup>1</sup>H NMR (CDCl<sub>3</sub>):  $\delta$  = 8.44, 8.23, 8.01, 7.89, 7.73, 7.55 (6d, 1 + 1 + 1 + 1 + 1 + 1H,  $J$  = respectively, 4.8, 4.8, 5.1, 4.8, 4.8, 5.1 Hz, pyrrole), 7.99 (d, 1H,  $J$  = 9 Hz, cyclized phenyl), 7.75 (broad signal, 2H, aryl), 7.65–7.3 (m, 18H, 16 aryl + 2 cyclized phenyl), 2.57, 2.53, 2.44, 2.42 (4s, 3 + 3 + 3 + 3H, methyl). UV–visible (CH<sub>2</sub>Cl<sub>2</sub>):  $\lambda$  = 464 nm ( $\epsilon$  = 85 000), 658 (23 800), 690 (30 700). HRMS: calcd for C<sub>55</sub>H<sub>38</sub>N<sub>4</sub>O<sub>2</sub>Ni+H<sup>+</sup>, 845.2421; found, 845.2373.

**Corrole 24.** <sup>1</sup>H NMR (CDCl<sub>3</sub>):  $\delta$  = 7.61 (broad d, 2H,  $J$  = 7.5 Hz, benzoate *o*-H), 7.57 (d, 1H,  $J$  = 8.7 Hz, cyclized phenyl), 7.52 (broad t, 1H,  $J$  = ca. 8 Hz, benzoate *p*-H), 7.32 (dd, 2H,  $J$  = 7.5 Hz, benzoate *m*-H), 7.30–7.12 (m, 11H, 10 aryl + 1 pyrrole), 6.81 (dd, 1H,  $J$  = 8.7 and 1.8 Hz, cyclized phenyl), 6.66 (d, 1H,  $J$  = 1.8 Hz, cyclized phenyl), 6.65 (d,  $J$  = 5.1 Hz, pyrrole), 6.61 (d,

2H,  $J$  = 8.4 Hz, aryl), 6.16, 6.00, 5.92, 5.85 (4d, 1 + 1 + 1 + 1H,  $J$  = respectively, 4.8, 4.5, 4.8, 4.5 Hz, pyrrole), 3.44 (s, 3H, methoxy), 2.40, 2.36, 2.04 (3s, 3 + 3 + 3H, methyl). UV–visible (CH<sub>2</sub>Cl<sub>2</sub>):  $\lambda$  = 388 nm ( $\epsilon$  = 65 000), 466 (36 000), 488 (38 500), 600 (28 000), 702 (13 800), 758 (23 800). HRMS: calcd for C<sub>55</sub>H<sub>38</sub>N<sub>4</sub>O<sub>3</sub>Ni+H<sup>+</sup>, 861.2370; found, 861.2371.

**Corrole 25.** <sup>1</sup>H NMR (CDCl<sub>3</sub>):  $\delta$  = 7.65 (broad d, 1H,  $J$  = 8.6 Hz, cyclized phenyl), 7.61 (dd, 2H,  $J$  = 8 and 1 Hz, benzoate *o*-H), 7.53 (tt, 1H,  $J$  = 7.8 and 1.5 Hz, benzoate *p*-H), 7.45–7.3 (m, 13H, 12 aryl + 1 pyrrole), 7.14 (d, 2H,  $J$  = 9 Hz, methoxyphenyl), 6.97 (dt, 1H,  $J$  = 8.6 and 1.5 Hz, cyclized phenyl), 6.91 (dd, 1H,  $J$  = 7.8 and 1.5 Hz, cyclized phenyl), 6.67 (dt, 1H,  $J$  = 7.8 and 1.5 Hz, cyclized phenyl), 6.64 (d, 1H,  $J$  = 5 Hz, pyrrole), 6.61 (d, 2H,  $J$  = 9 Hz, methoxyphenyl), 6.15, 6.00, 5.91, 5.88 (4d, 1 + 1 + 1 + 1H,  $J$  = 5 Hz, pyrrole), 3.45 (s, 3H, methoxy). UV–visible (CH<sub>2</sub>Cl<sub>2</sub>):  $\lambda$  = 384 nm ( $\epsilon$  = 54 000), 460 (32 500), 488 (32 000), 598 (23 300), 696 (12 200), 758 (18 700). HRMS: calcd for C<sub>52</sub>H<sub>32</sub>N<sub>4</sub>O<sub>3</sub>Ni+H<sup>+</sup>, 819.1901; found, 819.1912.

**Quenching of the Brown Acylation Solution with NaOH.** Porphyrin **4** (300 mg; 0.33 mmol) was acylated with benzoic anhydride according to method C. To the resulting dark brown solution was added chlorobenzene (20 mL) followed by sodium hydroxide (10 wt % aqueous solution, 50 mL), and the two-phase mixture was vigorously stirred for 15 min. The organic phase was decanted, washed with water (2 × 100 mL), and dried over Na<sub>2</sub>SO<sub>4</sub>. After evaporation, the residue was chromatographed (alumina, 400 mL in toluene) to give successively a dimeric fraction (39 mg from toluene + methanol; impure, see below), brown alcohol **28** (72 mg; 21%), and green alcohol **29** (84 mg; 25%), both crystallized from CH<sub>2</sub>Cl<sub>2</sub>–MeOH.

The NMR spectrum of the dimeric fraction **30** in deuterated benzene showed eight singlets for the *tert*-butyl groups (1.54, 1.50, 1.48, 1.38, 1.35, 1.28, 1.05, 0.99 ppm) as well as a series of doublets due to pyrrolic protons between 9.2 and 5.9 ppm, in addition to signals due to alcohol **29** and other impurities. In MS, we detected for dimer **30** a peak cluster corresponding to C<sub>134</sub>H<sub>126</sub>N<sub>8</sub>ONi<sub>2</sub> + H<sup>+</sup>.

**Alcohol 28.** <sup>1</sup>H NMR (CDCl<sub>3</sub>):  $\delta$  = 9.47, 8.87 (2d, 1 + 1H,  $J$  = 5.1 Hz, pyrrole), 8.73 (s, 1H, pyrrole), 8.65, 8.63, 8.60, 8.58 (4d, 1 + 1 + 1 + 1H,  $J$  = 5.1 Hz, pyrrole), 8.07 (d, 1H,  $J$  = 1.8 Hz, cyclized phenyl), 7.95–7.6 (broad m, 4H, aryl), 7.89 (d, 1H,  $J$  = 8.4 Hz, cyclized phenyl), 7.75–7.6 (m, 10H, aryl), 7.56 (dd, 1H,  $J$  = 8.4 and 1.8 Hz, cyclized phenyl), 7.16–7.24 (m, 3H, phenyl on six-membered ring *m*- and *p*-H), 3.14 (s, 1H, OH), 1.56, 1.54, 1.53, 1.40 (4s, 9 + 9 + 9 + 9H, *tert*-butyl). UV–visible (CH<sub>2</sub>Cl<sub>2</sub>):  $\lambda$  = 442 nm ( $\epsilon$  = 220 000), 558 (18 000), 600 (14 000). HRMS: calcd for C<sub>67</sub>H<sub>64</sub>N<sub>4</sub>ONi+H<sup>+</sup>–H<sub>2</sub>O, 981.4401; found, 981.4373.

**Alcohol 29.** <sup>1</sup>H NMR (CDCl<sub>3</sub>):  $\delta$  = 8.90 (d, 1H,  $J$  = 5.1 Hz, pyrrole), 8.62 (d, 1H,  $J$  = 8.4 Hz, cyclized phenyl), 8.52, 8.23, 8.08, 8.05, 7.91 (5d, 1 + 1 + 1 + 1H,  $J$  = respectively, 5.1, 4.8, 4.8, 4.8, 4.8 Hz, pyrrole), 7.85 (dd, 1H,  $J$  = 8.4 and 1.8 Hz, cyclized phenyl), 7.81 (d, 1H,  $J$  = 1.8 Hz, cyclized phenyl), 7.85–7.55 (m, 17H, aryl), 6.66 (d, 1H,  $J$  = 4.5 Hz, chlorinic H), 2.33 (d, 1H,  $J$  = 4.5 Hz, OH), 1.52, 1.49, 1.45, 1.37 (4s, 9 + 9 + 9 + 9H, *tert*-butyl). UV–visible (CH<sub>2</sub>Cl<sub>2</sub>):  $\lambda$  = 448 nm ( $\epsilon$  = 182 000), 616 (19 200), 666 (32 200). HRMS: calcd for C<sub>67</sub>H<sub>64</sub>N<sub>4</sub>ONi+H<sup>+</sup>–H<sub>2</sub>O, 981.4401; found, 981.4407.

**Conversion of Ketone 9 into Corrole 38.** To a solution of ketone **9** (40 mg; 0.056 mmol) in dry CH<sub>2</sub>Cl<sub>2</sub> (8 mL) was added CuI (8 mg; 0.042 mmol) followed by a solution of phenylmagnesium bromide (0.66 mmol in 4 mL of diethyl ether) added over 2 min. TLC checking showed that full transformation of the starting material had occurred. The reaction mixture was diluted with CH<sub>2</sub>Cl<sub>2</sub> (100 mL) and poured into aqueous HCl (250 mL; 2 M). The organic phase was washed with water (3 × 500 mL), dried over Na<sub>2</sub>SO<sub>4</sub>, and evaporated. To the residue were added benzoic anhydride (80 mg; 0.082 mmol), (dimethylamino)pyridine (10 mg; 0.082 mmol), and pyridine (10 mL). The solution was stirred under

dry air for 1 h and then evaporated under vacuum. Toluene (3 × 10 mL) was added and evaporated under reduced pressure to eliminate the last traces of pyridine. The residue was chromatographed (silica gel; 75 mL in toluene). Elution with the same solvent gave corrole **38** (5 mg; 10%) after crystallization from CH<sub>2</sub>Cl<sub>2</sub>–MeOH.

**Corrole 38.** <sup>1</sup>H NMR (CDCl<sub>3</sub>): δ = 7.63 (d, 1H, *J* = 8.4 Hz, cyclized phenyl), 7.50–7.55 (m, 3H, phenyl), 7.20–7.40 (m, 16H, 15 phenyl + 1 pyrrole H), 7.12 (t, 2H, *J* = 8.1 Hz, phenyl), 6.95 (tt, 1H, *J* = 9, 1.5, and 1.5 Hz, phenyl *p*-H), 6.81 (dd, 1H, *J* = 8.4 and 1 Hz, cyclized phenyl), 6.66 (ddd, 1H, *J* = 9, 9, and 1 Hz, cyclized phenyl), 6.63 (d, 1H, *J* = 5 Hz, pyrrole), 6.12 (d, 1H, *J* = 5.1 Hz, pyrrole), 5.97 (d, 1H, *J* = 4.5 Hz, pyrrole), 5.89 (d, 1H, *J* = 5.1 Hz, pyrrole), 5.83 (d, 1H, *J* = 4.5 Hz, pyrrole). UV–visible (CH<sub>2</sub>Cl<sub>2</sub>): λ = 384 nm (ε = 48 500), 488 (27 000), 552 (sh., 12 000), 596 (19 500), 700 (82 000), 760 (14 700). HRMS: calcd for C<sub>51</sub>H<sub>30</sub>N<sub>4</sub>O<sub>2</sub>Ni+H<sup>+</sup>, 789.1795; found, 789.1748.

**Preparation of Hydroxyporphyrins 32 or 37 from Ketones 6 or 36.** A solution of ketone **6** (105 mg; 0.105 mmol) and tetra-*n*-butylammonium borohydride (100 mg; 0.37 mmol) in benzene (30 mL) was stirred for 16 h (at mid reaction, an additional 25 mg (0.1 mmol) of borohydride was added). The solution was concentrated to 3 mL at 20 °C under reduced pressure, and MeOH (5 mL) was added. The solution was again concentrated to 3 mL, and a further 5 mL of MeOH was added. The fine purple precipitate was filtered, washed thoroughly with MeOH, and dried under vacuum (90 mg; 86%). Under the same conditions, the corresponding palladium ketone **36**<sup>13</sup> gave hydroxyporphyrin **37** in 90% yield. Both compounds, in particular, the palladium complex **37**, slowly oxidized, even in the solid state, to give ketones **6** or **36** as the major product. Their purity was checked by NMR and TLC, and they were used as such for the next step.

**Nickel Hydroxyporphyrin 32.** <sup>1</sup>H NMR (CDCl<sub>3</sub>): δ = 9.97, 8.90, 8.66, 8.62, 8.61, 8.39 (6d, 1 + 1 + 1 + 1 + 1 + 1H, *J* = 5 Hz, pyrrole), ca. 8.3 (broad signal, 1H, aryl), 7.9 (broad signal, 3H, aryl), 7.84 (d, 1H, *J* = 8.4 Hz, cyclized phenyl), 7.7–7.5 (m, 9H, aryl), 7.4 (broad signal, 1H, aryl), 7.25–7.1 (m, 5H, aryl), 6.09 (s, 1H, CH on six-membered ring), 5.80 (s, 1H, OH), 1.56, 1.53, 1.51, 1.37 (4s, 9 + 9 + 9 + 9H, *tert*-butyl). UV–visible (CH<sub>2</sub>Cl<sub>2</sub>): λ = 436 nm (ε = 202 000), 556 (13 900), 596 (14 200).

**Palladium Hydroxyporphyrin 37.** <sup>1</sup>H NMR (CDCl<sub>3</sub>): δ = 9.65, 8.86, 8.72, 8.71, 8.69, 8.39 (6d, 1 + 1 + 1 + 1 + 1 + 1H, *J* = 5 Hz, pyrrole), 8.7 (broad signal, 1H, aryl), 8.28 (d, 2H, *J* = 8 Hz, aryl), 8.19 (d, 1H, *J* = 7.8 Hz, cyclized phenyl), 7.9–7.6 (m, 11H, aryl), 7.54 (d, 2H, *J* = 8 Hz, phenyl *o*-H), 7.15–7.05 (m, 3H, phenyl *m* + *p*-H), 6.26 (s, 1H, CH on six-membered ring), 5.94 (s, 1H, OH), 1.61, 1.58, 1.54, 1.44 (4s, 9 + 9 + 9 + 9H, *tert*-butyl). UV–visible (CH<sub>2</sub>Cl<sub>2</sub>): λ = 436 nm (ε = 211 000), 546 (16 500), 590 (18 300).

**Conversion of Nickel Hydroxyporphyrin 32 into Corrole 7 and Byproducts 6, 8, 34, and 35.** To hydroxyporphyrin **32** (90 mg) were added benzoic anhydride (625 mg; 5 mmol), DMAP (50 mg; 0.41 mmol), and pyridine (25 mL). The solution was stirred under dry air. It turned rapidly green and then dark olive-green. After 2.5 h, the solution was treated as above (method A) and products **7** (24%), **6** (27%), **8** (5%), **34** (5%), and **35** (4%) were eluted successively and were crystallized from CH<sub>2</sub>Cl<sub>2</sub>–MeOH.

**Hydroxyester 34.** <sup>1</sup>H NMR (50 °C, CDCl<sub>3</sub>): δ = 9.46, 8.86, 8.65, 8.59, 8.53, 8.45 (6d, 1 + 1 + 1 + 1 + 1 + 1H, *J* = respectively, 4.8, 4.8, 5.1, 5.1, 5.4, 5.4 Hz, pyrrole), 7.94, 7.70 (2d, 2 + 2H, *J* = 8 Hz, *meso*-aryl next to benzoate), 7.87 (d, 2H, *J* = 8 Hz, aryl), 7.85 (d, 1H, *J* = 8 Hz, cyclized phenyl), 7.65–7.5 (m, 12H, aryl), 7.33 (dd, 2H, *J* = 7.8 Hz, aryl *meta*-H), 7.13 (very broad d, 1H, aryl), 6.98–7.04 (m, 3H, aryl), 4.12 (s, 1H, OH), 1.54, 1.46, 1.28, 1.03 (4s, 9 + 9 + 9 + 9H, *tert*-butyl). UV–visible (CH<sub>2</sub>Cl<sub>2</sub>): λ = 442 nm (ε = 116 000), 560 (7400), 600 (5900). HRMS: major peak cluster, calcd for C<sub>74</sub>H<sub>68</sub>N<sub>4</sub>O<sub>3</sub>Ni + H<sup>+</sup>–H<sub>2</sub>O, 1101.4612; found, 1101.4627; minor peak cluster, calcd for C<sub>74</sub>H<sub>68</sub>N<sub>4</sub>O<sub>3</sub>Ni + Na<sup>+</sup>, 1141.4537; found, 1141.4548.

**Corrole 35.** <sup>1</sup>H NMR (60 °C, C<sub>2</sub>D<sub>2</sub>Cl<sub>4</sub>): δ = 7.75 (d, 1H, *J* = 9 Hz, cyclized phenyl), 7.54 (d, 1H, *J* = 5.1 Hz, pyrrole), 7.46 (2 superimposed d, 4H, *J* = 8 Hz, aryl), 7.42–7.38 (m, 3H, aryl), 7.35–7.3 (m, 4H, aryl), 7.22 (d, 2H, *J* = 7.5 Hz, aryl), 7.17 (dd, 1H, *J* = 9 and 2 Hz, cyclized phenyl), 7.1–7.05 (m, m, 3H, aryl), 6.96 (d, 2H, *J* = 8 Hz, aryl), 6.93 (d, 1H, *J* = 5.1 Hz, pyrrole), 6.88 (d, *J* = 2 Hz, cyclized phenyl), 6.45 (d, 1H, *J* = 4.8 Hz, pyrrole), 6.35 (s, 1H, pyrrole), 6.19 (d, 1H, *J* = 4.8 Hz, pyrrole), 1.41, 1.33, 1.31, 1.11 (4s, 9 + 9 + 9 + 9H, *tert*-butyl); the remaining aryl protons (4H) show as very broad signals between 7.15 and 7.4 ppm. UV–visible (CH<sub>2</sub>Cl<sub>2</sub>): λ = 394 nm (ε = 50 500), 470 (sh., 26 000), 492 (38 200), 600 (21 500), 698 (12 200), 762 (19 800). HRMS: calcd for C<sub>74</sub>H<sub>66</sub>N<sub>4</sub>O<sub>3</sub>Ni + H<sup>+</sup>, 1117.4561; found, 1117.4604.

**Acknowledgment.** We thank André Decian for solving the crystal structures and Patrick Wehrung for the mass spectra.

**Supporting Information Available:** General experimental procedures. X-ray crystallographic information files (CIF) for compounds **10** and **12**. Preliminary crystal structure report for the *meso*-tolyl analogue of **35**. Cyclic voltammetry data for compound **31**. This material is available free of charge via the Internet at <http://pubs.acs.org>.

JO0600499